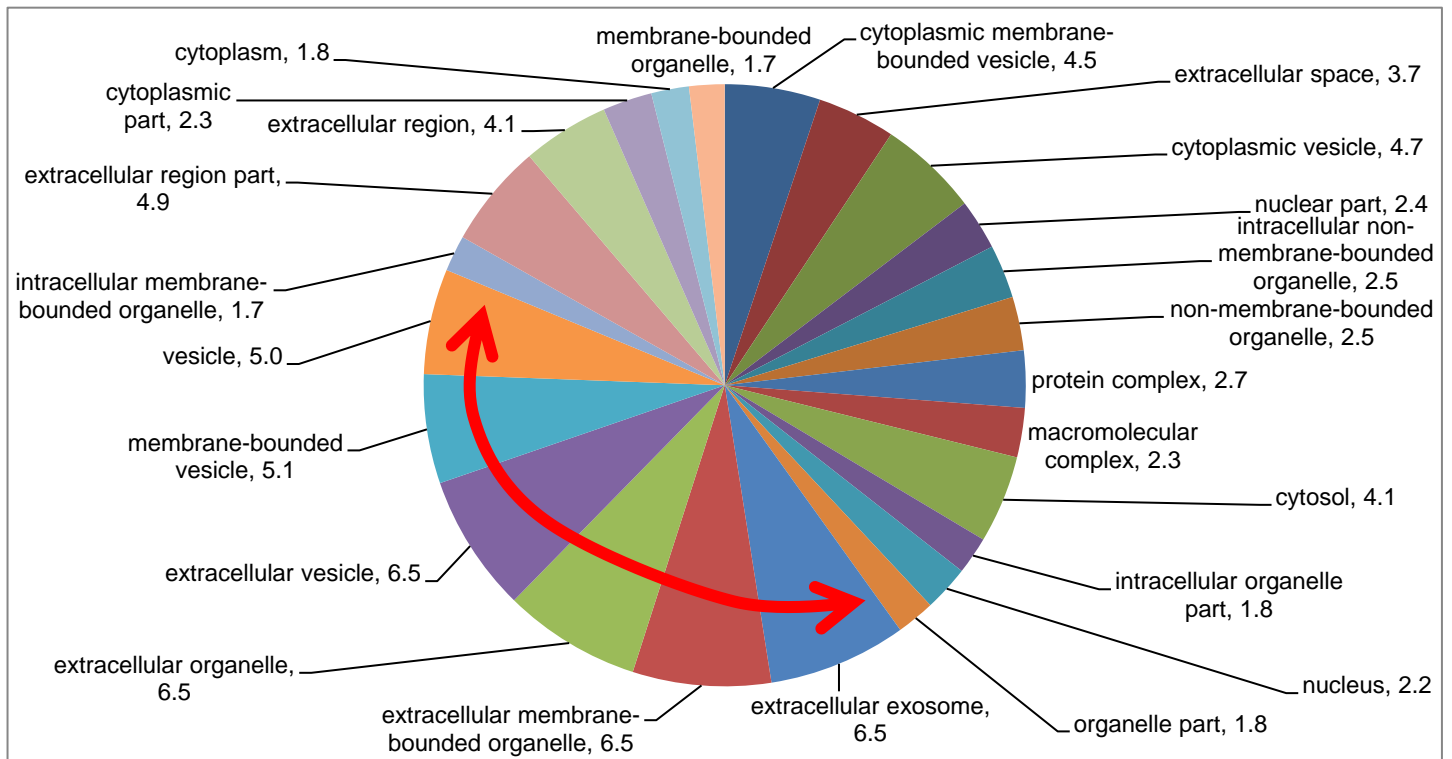


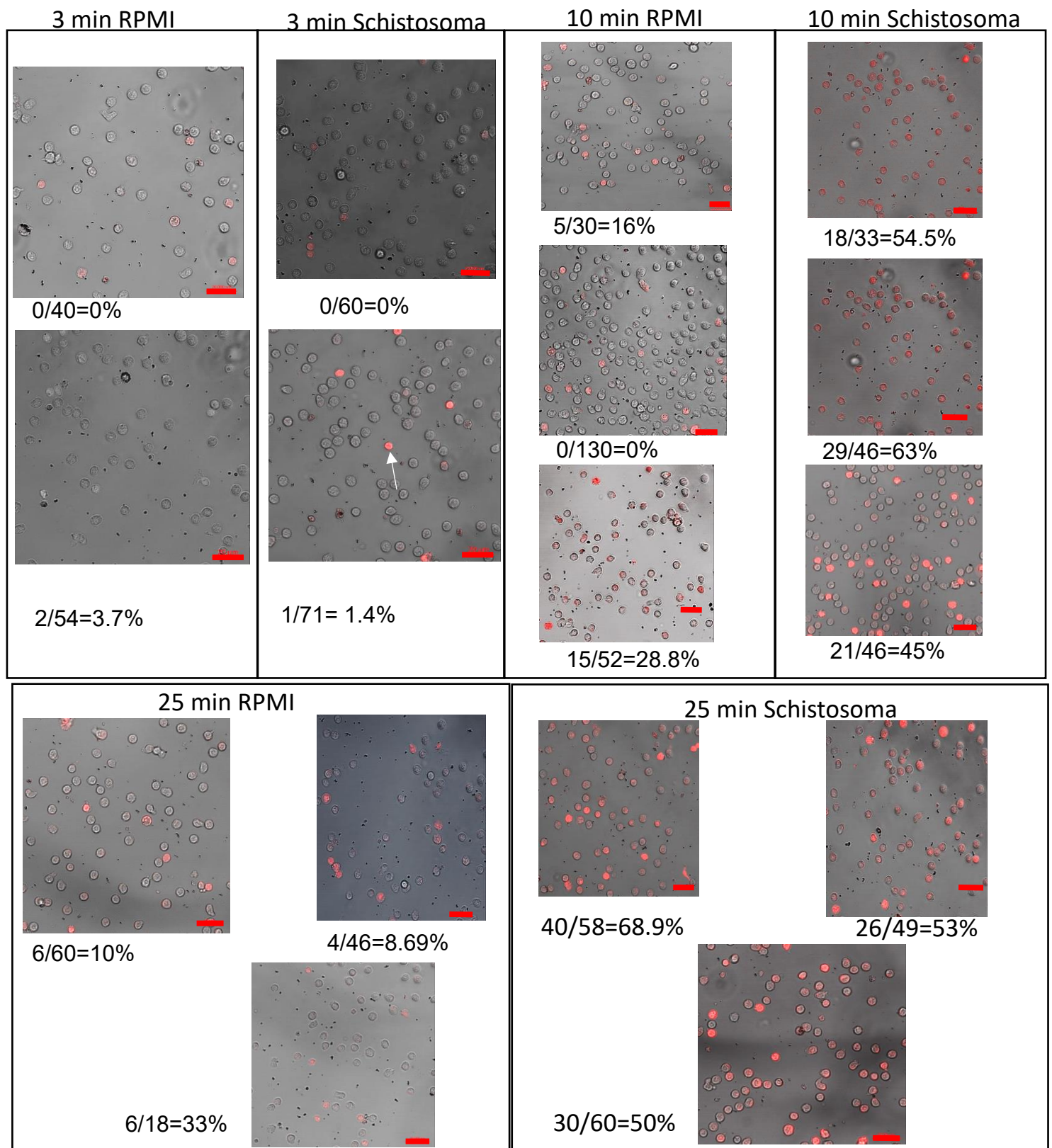
Schistosomal extracellular vesicle-enclosed miRNAs modulate host T helper cell differentiation

Contents of Appendix files

Appendix file	Title	page
Appendix Figure S1	Predicted cellular component of the identified proteins in the proteomics by GO Ontology analysis software	2
Appendix Figure S2	images of uptake of EVs by CD4 cells	3
Appendix Figure S3	Detection of miR-10 and Bantam in the same fractions with the schistosomal-EVs density sucrose gradient.	4
Appendix Figure S4	Uptake of schistosomal-labeled EVs and schistosomal-miRNAs by Jurkat cells	5
Appendix Figure S5	Schistosoma miR-10 putative targets analysis	6
Appendix Figure S6	Three Western blot assays, using anti-MAP3K7 or GAPDH antibodies, for protein extracts from Th cells that were either exposed or not exposed to the Schistosomes	7
Appendix Figure S7	Three Western blot assays, using anti-MAP3K7 or GAPDH antibodies, for protein extracts from Jurkat cells overexpressing miR-10 or control plasmid	7
Appendix Table S1:	FunRich bioinformatic analysis of the distribution of the identified schistosomal-proteins in cellular components.	8
Appendix Table S2	Genes that were downregulated in the presence of Schistosomes, and are known to be regulated by NF- κ B.	9
Appendix Table S3	Genes that were downregulated in the presence of Schistosomes and are known as NF- κ B activators	10
References to appendix table S2 and S3		10-12

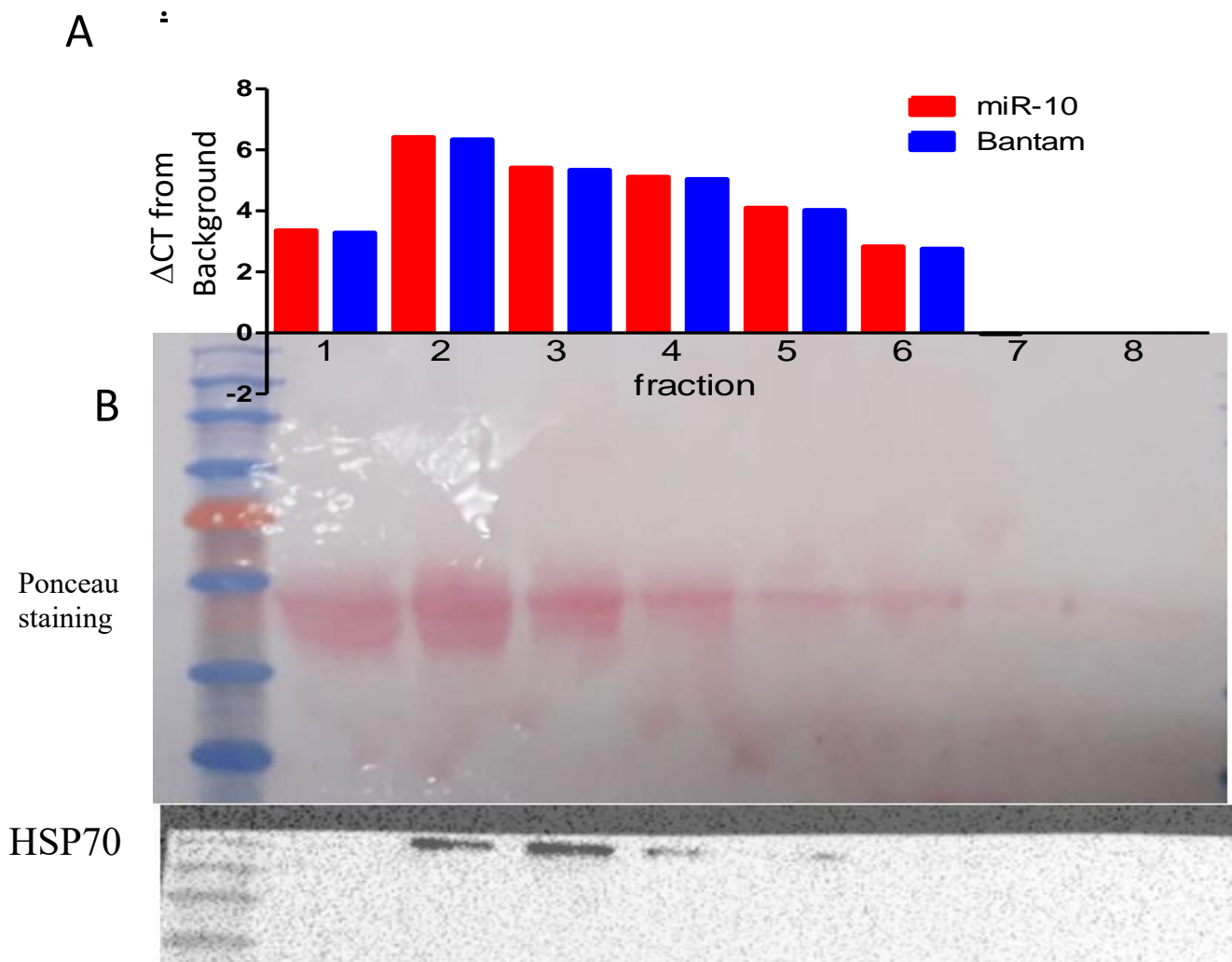


Appendix Figure S1: predicted cellular component of the identified proteins in the proteomics by GO Ontology analysis software. Only results with $P < 0.05$ (calculated by Bonferroni correction for multiple testing) are displayed. Only cellular components that were predicted to have more than 3 proteins are displayed. The numbers present the fold enrichment. The red arrow indicates organelles that are extracellular vesicles.

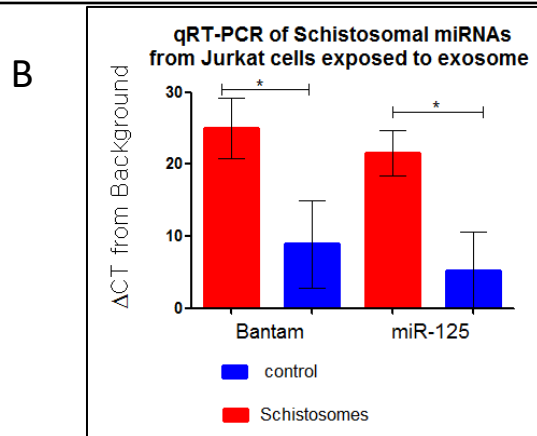
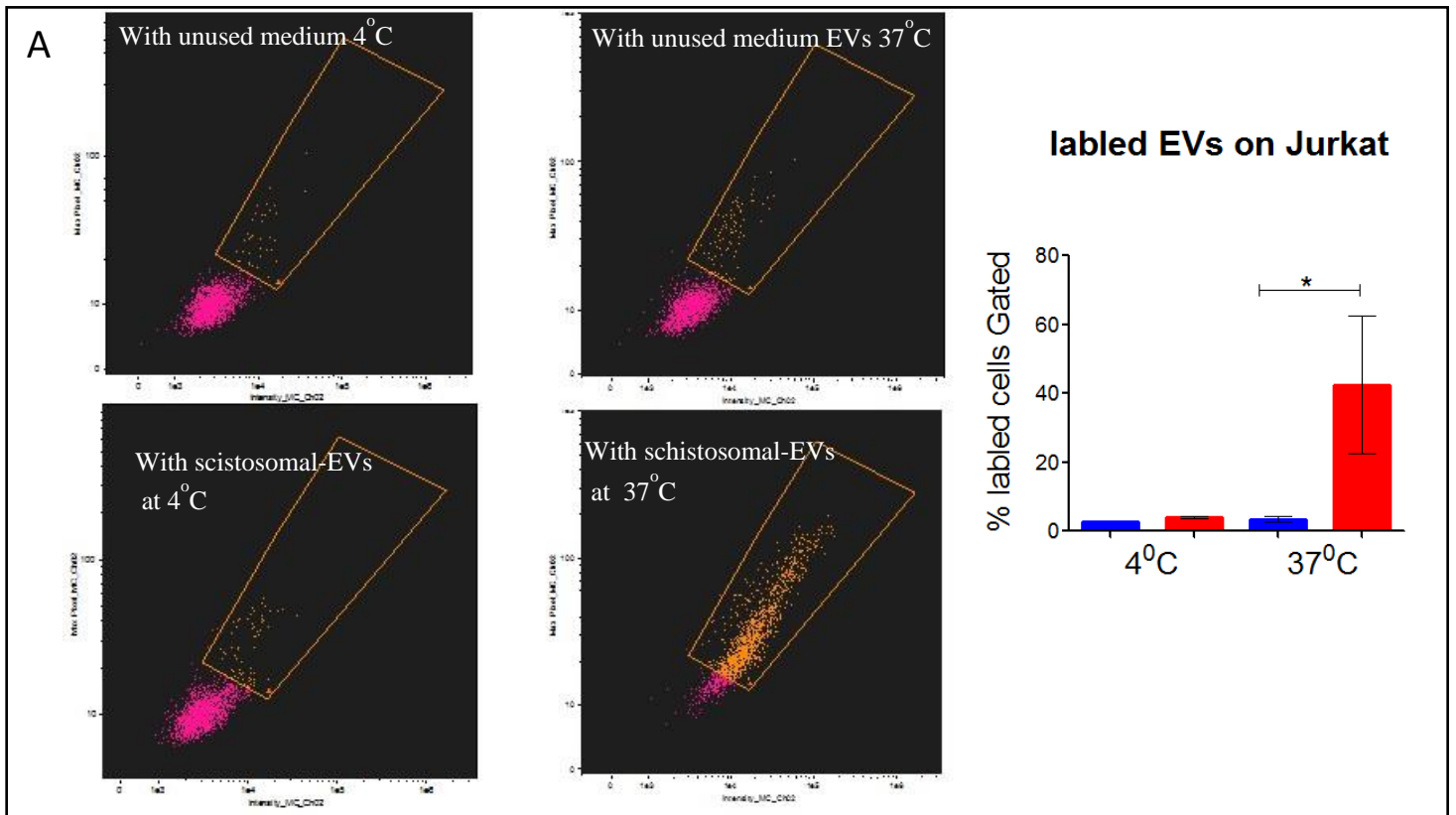


Appendix Figure S2: images of uptake of EVs by CD4 cells, in each image the calculation of percentage of labeled cells in a taken image is shown. The red line represent of $20\mu\text{m}$.

The EVs were stain with Thiazole Orange as written in the Materials and Methods. To avoid a high background staining, after the labeling, the EVs were washed in ~ 70 ml RPMI. Still there are traces of non-EVs color residues in the control that probably stained cells with a defective cytoplasmatic membrane that looks totally different from EV-staining cells. Obviously, these cells were not counted (the white arrow that is shown in image 3 min Schistosoma lower image mark example of none specific staining).



Appendix Figure S3: Detection of miR-10 and Bantam in the same fractions with the schistosomal-EVs in density sucrose gradient EVs were isolated from 100ml Schistosomal growing medium. The EVs were concentrated into 500 μ l of PBS, then loaded onto the top OptiPrep™ density sucrose gradient (see Methods). After centrifugation, 8 fractions of 1ml were collected (from top to bottom). From each fraction, RNA and proteins were extracted and subjected to: A) qRT-PCR using specific primers to Schistosomal-miRNAs, Bantam and miR-10-5p. B) Ponceau staining and Western blot analysis using anti-human HSP70 antibodies (since there are no available antibodies recognizing any Schistosomal-EV proteins, and the identity between human and Schistosomal-hsp-70 is 83%).



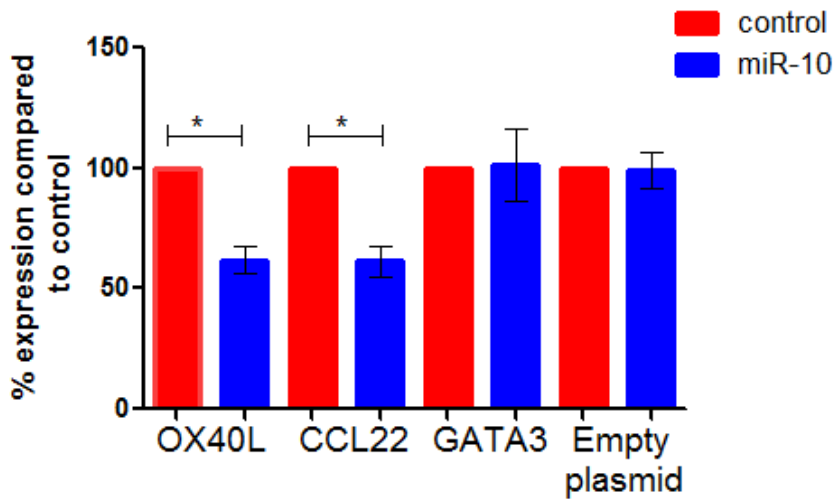
Appendix Figure S4: Uptake of schistosomal-labeled EVs and schistosomal-miRNAs by Jurkat cells. **A)** EVs were purified from culture medium where the Schistosomes grew in or from fresh unused medium. Both were stained using Thiazole Orange. $\sim 5 \times 10^6$ purified EVs were incubated with 1×10^6 cells for 10min at 37°C or 4°C. EV-uptake was detected by image stream flow cytometry (IFC). The mean \pm SEM was calculated from 3 independent experiments. Statistics were performed using Mann Whitney t-test ($*p < 0.05$). **B)** $\sim 5 \times 10^6$ purified EVs were added to 1×10^6 Jurkat cells for 48h. RNA was extracted and subjected to qRT-PCR with specific primers to Schistosomal-miR-Bantam or schistosomal-miR-125. The data are presented as the delta Ct from average control background. The mean \pm SEM was calculated from 3 independent experiments. Statistics were performed using Unpaired t-test with Welch's correction ($*p < 0.05$)

A

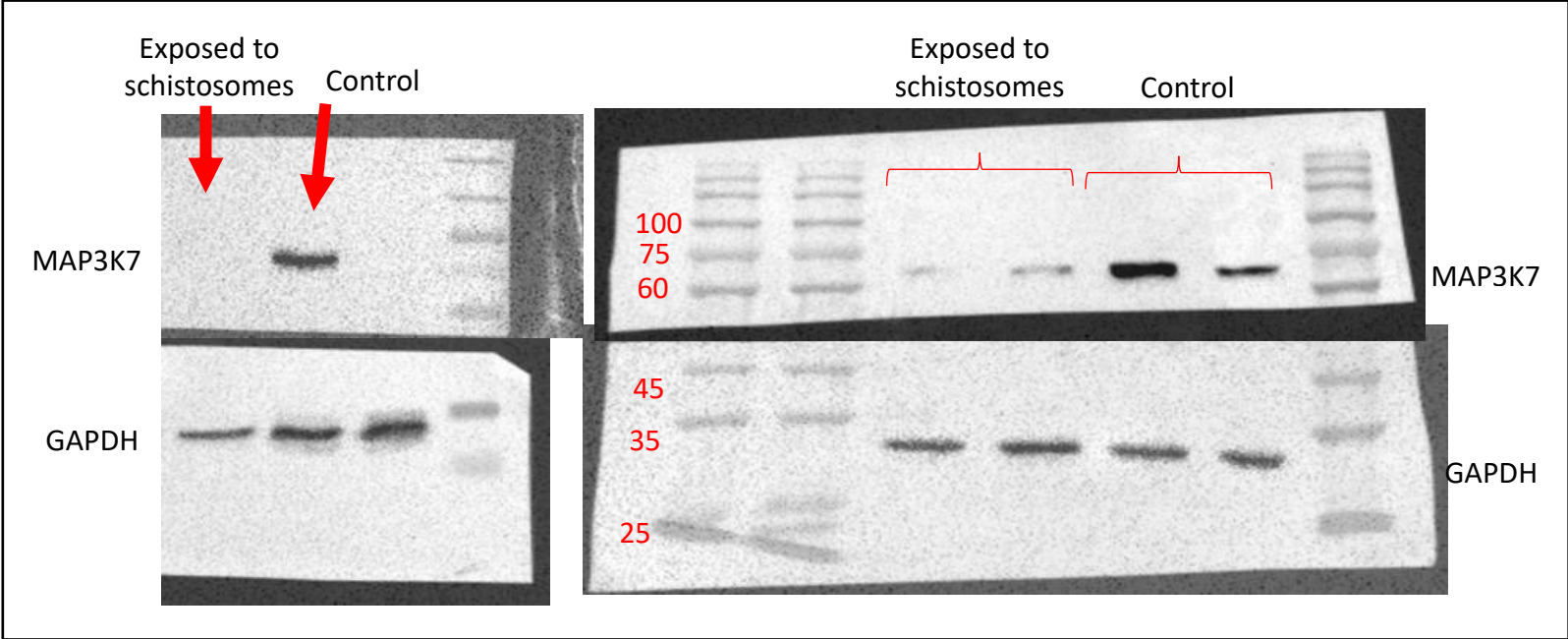
Position 826-832 of TNFSF4 3' UTR	5' ...GGGAACUGGACAUCUCAGGGUAA...
<i>Schistosoma</i> miR-10a-5p	3' GGUUUGAGCCCAGAUGUCCCAA
Position 2274-2280 of CCL22 3' UTR	5' ...GCUGGUGCCGCUCUCAGGGUAA...
<i>Schistosoma</i> miR-10a-5p	3' GGUUUGAGCCCAGAUGUCCCAA
Position 236-242 of GATA3 3' UTR	5' ..CAUAUCCCCUAUUUAACAGGGUC...
<i>hsa-miR-10a-5p</i>	3' GGUUUGAGCCCAGAUGUCCCAA

B

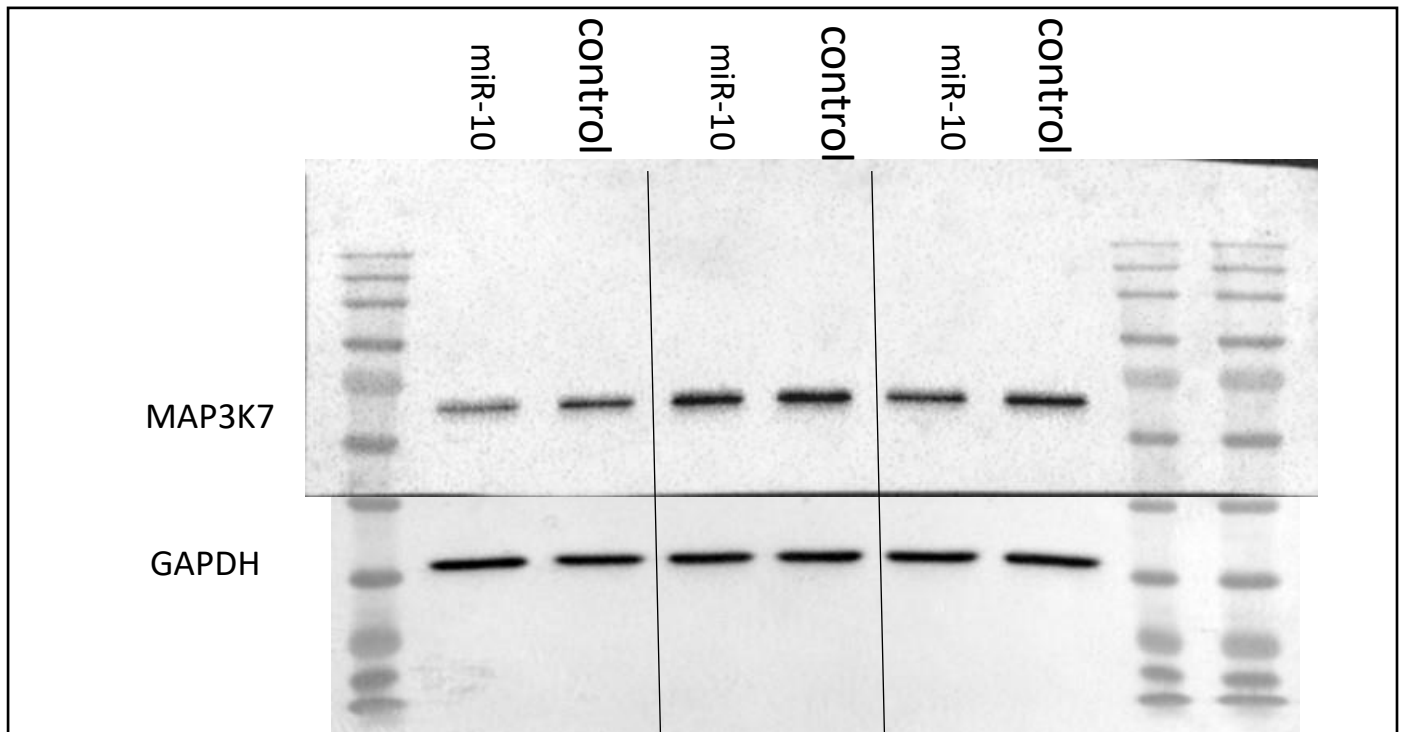
Effect of miR-10 on putative targets



Appendix Figure S5: Schistosoma miR-10 putative targets analysis A) The putative binding sites of miR-10 on *OX40L* (TNFSF4), *CCL22* and *GATA3* 3' UTR are shown (taken from TargetScan at http://www.targetscan.org/vert_72/). (B) Human Jurkat cells stably expressing Schistosomal-miR-10 were transfected with either psiCHECK-II vector (empty plasmid), psiCHECK-OX40L-3'UTR-luciferase, psiCHECK-II-CCL22-3'UTR-luciferase or psiCHECK-II-GATA3-3'UTR-luciferase. 24h after transfection the cells lysates were subjected to luciferase assay. The results are presented as the ratio of expression of renilla/luciferase that was normalized relative to Jurkat cell transfected with control vector not expressing miR-10. Values are expressed as the mean+SD of at least 3 independent experiments. Statistics were performed using t-test *p<0.05.



Appendix Figure S6: Three Western blot assays, using anti-MAP3K7 or GAPDH antibodies, for protein extracts from Th cells that were either exposed or not exposed to the Schistosomes.



Appendix Figure S7: Three Western blot assays, using anti-MAP3K7 or GAPDH antibodies, for protein extracts from Jurkat cells overexpressing miR-10 or control plasmid

Appendix Table S1: FunRich bioinformatic analysis of the distribution of the identified schistosomal-proteins in cellular components

Cellular component	No. of proteins out of the 59 proteins mapped to the specific cellular component *	Expected Percentage of proteins in specific cellular component out of the data set of 28328 proteins display	Percentage of protein found in our proteomics	Corrected p-value **
Exosomes	45	7.1	76.27	1.71E-25
Lysosome	33	19.88	55.93	3.35E-15
Centrosome	19	5.7	32.20	1.64E-10
Cytoplasm	45	20.4	76.27	3.62E-07
Cytosol	19	2.2	32.20	5.109E-06
Proteasome complex	4	4.1	6.78	0.000581
Intracellular ferritin complex	2	12.2	3.39	0.000891
Proteasome core complex	2	4.42	3.39	0.0053
Microtubule	5	6.38	8.47	0.00911
Perinuclear region	5	4.3	8.47	0.01053
Mitochondrion	14	1.5	23.72	0.0226
Cytoskeleton	7	0.45	11.86	0.091
Nucleolus	12	0.46	20.34	0.195
Nucleosome	2	3.9	3.39	0.251
Nucleus	33	0.12	55.93	0.524
Eukaryotic translation elongation factor 1 complex	1	1.23	1.69	0.66

*Out of 84 proteins presented in FunRich analysis software, 59 could be mapped to a specific predicted cellular component. In the table are displayed cellular component with more than 1.5% of the 59 proteins ** (Bonferroni method).

Appendix Table S2: Genes that were downregulated in the presence of Schistosomes, and are known to be regulated by NF-κB.				
Gene symbol	Fold change Schistosoma/ control	P value t-test	Reference	
Mmp7	0.036	5.8685E-06	(1, 2)	
Pld1	0.037	6.60044E-06	(3)	
Olr1	0.085	0.00021079	(4)	
Ngb	0.085	0.00021079	(5)	
Plcb1	0.149	0.002303683	(6)	
Aire	0.198	0.003921811	(7)	
Serpine2	0.307	0.000703478	(8)	
Cx3cr1	0.318	0.006648255	(9)	
Mmp10	0.425	3.22662E-05	(10)	
Alpl (TNAP)	0.476	0.000848196	(11)	
IL-10	0.477	0.000753686	(12)	
Tnfsf4 (OX40L)	0.483	0.00358029	(13)	
Spp1 (osteopontin)	0.484	0.007954298	(14)	
Aqp9 (aquaporin 9)	0.490	0.010170549	(15)	
Prkcdbp	0.491	0.029094084	(16)	
Ccl22	0.505	0.020326852	(17)	
Lhx2	0.513	0.024820865	(18)	
Cxcl2	0.523	0.034296724	(19)	
IL-2	0.537	0.03103846	(20)	
Clspn (Claspin)	0.552	0.000417044	(21)	
Pax6	0.565	0.002198222	(22)	
Inhba (activin)	0.565	0.002289994	(23)	
S100a6	0.587	0.000947966	(24)	
IL-13	0.588	0.005429866	(25)	
Ccne1(cyclin E1)	0.615	0.001209538	(26)	
Arg2(arginase II)	0.620	0.041714036	(27)	
Cd80 (B7.1)	0.621	0.04309922	(28)	
Crmp1	0.644	0.017272692	(29)	
IL-4	0.654	0.003695783	(30)	

Appendix Table S3: Genes that were downregulated in the presence of Schistosomes and are known as NF-κB activators			
Gene symbol	Fold change Schistosoma/ control	P value t-test	Reference
Matn2	0.059	4.67284E-05	(31)
Mapk15	0.105	0.000518879	(32)
Nos1	0.156	0.000278261	(33)
Hspb2	0.178	0.004999194	(34)
Plce1	0.237	0.00054487	(35)
Ch25h	0.289	0.034860576	(36)
Hmga2	0.372	0.014173237	(37)
Egf	0.383	0.016443394	(38)
Ripk4	0.403	0.00109687	(39)
Pth	0.404	0.000371483	(40)
Fgfr2	0.437	0.019419708	(41)
Ffar2	0.556	0.025468136	(42)
Rrm2	0.569	0.00041276	(43)
Il5ra	0.615	0.026085869	(44)
Prlr	0.616	0.016251622	(45)
Setd6	0.658	0.02201673	(46)

References to appendix table S2 and S3

1. Guan PP, et al. (2015) By activating matrix metalloproteinase-7, shear stress promotes chondrosarcoma cell motility, invasion and lung colonization. *Oncotarget* 6(11):9140-9159.
2. Liu JY, et al. (2017) Solute carrier family 12 member 5 promotes tumor invasion/metastasis of bladder urothelial carcinoma by enhancing NF-kappaB/MMP-7 signaling pathway. *Cell death & disease* 8(3):e2691.
3. Kang DW, et al. (2008) Phorbol ester up-regulates phospholipase D1 but not phospholipase D2 expression through a PKC/Ras/ERK/NFkappaB-dependent pathway and enhances matrix metalloproteinase-9 secretion in colon cancer cells. *J Biol Chem* 283(7):4094-4104.
4. Wang B, et al. (2017) Up-regulation of OLR1 expression by TBC1D3 through activation of TNFalpha/NF-kappaB pathway promotes the migration of human breast cancer cells. *Cancer Lett* 408:60-70.
5. Liu N, et al. (2012) Transcriptional regulation mechanisms of hypoxia-induced neuroglobin gene expression. *The Biochemical journal* 443(1):153-164.
6. Atef ME & Anand-Srivastava MB (2014) Enhanced expression of Gqalpha and PLC-beta1 proteins contributes to vascular smooth muscle cell hypertrophy in SHR: role of endogenous angiotensin II and endothelin-1. *Am J Physiol Cell Physiol* 307(1):C97-106.
7. Haljasorg U, et al. (2015) A highly conserved NF-kappaB-responsive enhancer is critical for thymic expression of Aire in mice. *Eur J Immunol* 45(12):3246-3256.
8. Suzuki S, et al. (2006) Identification of TNF-alpha-responsive NF-kappaB p65-binding element in the distal promoter of the mouse serine protease inhibitor SerpinE2. *FEBS letters* 580(13):3257-3262.
9. Xiao LJ, et al. (2012) Hypoxia increases CX3CR1 expression via HIF-1 and NFkappaB in androgen-independent prostate cancer cells. *International journal of oncology* 41(5):1827-1836.
10. Rothgiesser KM, Fey M, & Hottiger MO (2010) Acetylation of p65 at lysine 314 is important for late NF-kappaB-dependent gene expression. *BMC genomics* 11:22.

11. Henaut L, et al. (2016) TWEAK favors phosphate-induced calcification of vascular smooth muscle cells through canonical and non-canonical activation of NF-kappaB. *Cell death & disease* 7:e2305.
12. Liu YW, Chen CC, Tseng HP, & Chang WC (2006) Lipopolysaccharide-induced transcriptional activation of interleukin-10 is mediated by MAPK- and NF-kappaB-induced CCAAT/enhancer-binding protein delta in mouse macrophages. *Cell Signal* 18(9):1492-1500.
13. Arima K, et al. (2010) Distinct signal codes generate dendritic cell functional plasticity. *Science signaling* 3(105):ra4.
14. Partridge CR, He Q, Brun M, & Ramos KS (2008) Genetic networks of cooperative redox regulation of osteopontin. *Matrix Biol* 27(5):462-474.
15. Aharon R & Bar-Shavit Z (2006) Involvement of aquaporin 9 in osteoclast differentiation. *J Biol Chem* 281(28):19305-19309.
16. Lee JH, et al. (2011) Epigenetic alteration of PRKCDBP in colorectal cancers and its implication in tumor cell resistance to TNFalpha-induced apoptosis. *Clin Cancer Res* 17(24):7551-7562.
17. Poole E, et al. (2008) NF-kappaB-mediated activation of the chemokine CCL22 by the product of the human cytomegalovirus gene UL144 escapes regulation by viral IE86. *Journal of virology* 82(9):4250-4256.
18. Tomann P, Paus R, Millar SE, Scheidereit C, & Schmidt-Ullrich R (2016) Lhx2 is a direct NF-kappaB target gene that promotes primary hair follicle placode down-growth. *Development* 143(9):1512-1522.
19. Burke SJ, et al. (2014) NF-kappaB and STAT1 control CXCL1 and CXCL2 gene transcription. *Am J Physiol Endocrinol Metab* 306(2):E131-149.
20. Li Y, Ohms SJ, Sun C, & Fan J (2013) NF-kappaB controls Il2 and Csf2 expression during T cell development and activation process. *Mol Biol Rep* 40(2):1685-1692.
21. Kenneth NS, Mudie S, & Rocha S (2010) IKK and NF-kappaB-mediated regulation of Claspin impacts on ATR checkpoint function. *EMBO J* 29(17):2966-2978.
22. Yamanishi E, Yoon K, Alberi L, Gaiano N, & Mizutani K (2015) NF-kappaB signaling regulates the generation of intermediate progenitors in the developing neocortex. *Genes Cells* 20(9):706-719.
23. Wamsley JJ, et al. (2015) Activin upregulation by NF-kappaB is required to maintain mesenchymal features of cancer stem-like cells in non-small cell lung cancer. *Cancer Res* 75(2):426-435.
24. Joo JH, et al. (2003) Involvement of NF-kappaB in the regulation of S100A6 gene expression in human hepatoblastoma cell line HepG2. *Biochem Biophys Res Commun* 307(2):274-280.
25. Hinz M, et al. (2002) Nuclear factor kappaB-dependent gene expression profiling of Hodgkin's disease tumor cells, pathogenetic significance, and link to constitutive signal transducer and activator of transcription 5a activity. *J Exp Med* 196(5):605-617.
26. Chen JM, et al. (2015) The involvement of nuclear factor-kappaB in the nuclear targeting and cyclin E1 upregulating activities of hepatoma upregulated protein. *Cell Signal* 27(1):26-36.
27. Espanol A, Dasso M, Cella M, Goren N, & Sales ME (2012) Muscarinic regulation of SCA-9 cell proliferation via nitric oxide synthases, arginases and cyclooxygenases. Role of the nuclear translocation factor-kappaB. *Eur J Pharmacol* 683(1-3):43-53.
28. Zhao J, Freeman GJ, Gray GS, Nadler LM, & Glimcher LH (1996) A cell type-specific enhancer in the human B7.1 gene regulated by NF-kappaB. *J Exp Med* 183(3):777-789.
29. Gao M, et al. (2008) NF-kappaB p50 promotes tumor cell invasion through negative regulation of invasion suppressor gene CRMP-1 in human lung adenocarcinoma cells. *Biochem Biophys Res Commun* 376(2):283-287.
30. Li-Weber M, Giaisi M, Baumann S, Palfi K, & Krammer PH (2004) NF-kappa B synergizes with NF-AT and NF-IL6 in activation of the IL-4 gene in T cells. *Eur J Immunol* 34(4):1111-1118.
31. Li F, et al. (2017) ADAMTS5 Deficiency in Calcified Aortic Valves Is Associated With Elevated Pro-Osteogenic Activity in Valvular Interstitial Cells. *Arterioscler Thromb Vasc Biol* 37(7):1339-1351.
32. Wu DD, et al. (2017) Extracellular signal-regulated kinase 8-mediated NF-kappaB activation increases sensitivity of human lung cancer cells to arsenic trioxide. *Oncotarget* 8(30):49144-49155.
33. Baig MS, et al. (2015) NOS1-derived nitric oxide promotes NF-kappaB transcriptional activity through inhibition of suppressor of cytokine signaling-1. *J Exp Med* 212(10):1725-1738.
34. Sur R, Lyte PA, & Southall MD (2008) Hsp27 regulates pro-inflammatory mediator release in keratinocytes by modulating NF-kappaB signaling. *J Invest Dermatol* 128(5):1116-1122.
35. Li Y & Luan C (2018) PLCE1 Promotes the Invasion and Migration of Esophageal Cancer Cells by Up-Regulating the PKCalpha/NF-kappaB Pathway. *Yonsei Med J* 59(10):1159-1165.

36. Ichikawa T, et al. (2013) 25-hydroxycholesterol promotes fibroblast-mediated tissue remodeling through NF-kappaB dependent pathway. *Experimental cell research* 319(8):1176-1186.
37. Mantovani F, et al. (1998) NF-kappaB mediated transcriptional activation is enhanced by the architectural factor HMGI-C. *Nucleic Acids Res* 26(6):1433-1439.
38. Chung S, et al. (2017) Identification of EGF-NF-kappaB-FOXC1 signaling axis in basal-like breast cancer. *Cell Commun Signal* 15(1):22.
39. Meylan E, Martinon F, Thome M, Gschwendt M, & Tschopp J (2002) RIP4 (DIK/PKK), a novel member of the RIP kinase family, activates NF-kappa B and is processed during apoptosis. *EMBO reports* 3(12):1201-1208.
40. Cheng ZY, et al. (2018) Parathyroid hormone promotes osteoblastic differentiation of endothelial cells via the extracellular signal-regulated protein kinase 1/2 and nuclear factor-kappaB signaling pathways. *Experimental and therapeutic medicine* 15(2):1754-1760.
41. Tang CH, Yang RS, Chen YF, & Fu WM (2007) Basic fibroblast growth factor stimulates fibronectin expression through phospholipase C gamma, protein kinase C alpha, c-Src, NF-kappaB, and p300 pathway in osteoblasts. *J Cell Physiol* 211(1):45-55.
42. Lee SU, et al. (2013) beta-Arrestin 2 mediates G protein-coupled receptor 43 signals to nuclear factor-kappaB. *Biol Pharm Bull* 36(11):1754-1759.
43. Duxbury MS & Whang EE (2007) RRM2 induces NF-kappaB-dependent MMP-9 activation and enhances cellular invasiveness. *Biochem Biophys Res Commun* 354(1):190-196.
44. Lee EJ, Park SS, Kim WJ, & Moon SK (2012) IL-5-induced migration via ERK1/2-mediated MMP-9 expression by inducing activation of NF-kappaB in HT1376 cells. *Oncology reports* 28(3):1084-1090.
45. Olavarria VH, Sepulcre MP, Figueroa JE, & Mulero V (2010) Prolactin-induced production of reactive oxygen species and IL-1beta in leukocytes from the bony fish gilthead seabream involves Jak/Stat and NF-kappaB signaling pathways. *J Immunol* 185(7):3873-3883.
46. Mukherjee N, Cardenas E, Bedolla R, & Ghosh R (2017) SETD6 regulates NF-kappaB signaling in urothelial cell survival: Implications for bladder cancer. *Oncotarget* 8(9):15114-15125.